Evaluation of Sea Surface Temperature From the HY-2 Scanning Microwave Radiometer

Mingkun Liu, *Student Member, IEEE*, Lei Guan, *Member, IEEE*, Wei Zhao, and Ge Chen

Abstract—Haiyang-2 (HY-2) is the first marine dynamic environmental satellite of China, which was launched on August 16, 2011. The scanning microwave radiometer (RM) onboard HY-2 has low-frequency channels with the capability of observing sea surface temperature (SST) from space. In this paper, the Level 2A (L2A) SST products of HY-2 RM are evaluated. The global HY-2 RM L2A SST products are compared with the buoy SST measurements, WindSat SST, and National Oceanic and Atmospheric Administration Optimum Interpolation (OI) weekly SST products for the period from January 2012 to December 2014. The collocations of HY-2 RM, WindSat, and buoy SST data are generated with the spatial window of 0.25° and the temporal window of 0.5 h. The biases are −0.45 °C (RM minus buoy) and −0.41 °C (RM minus WindSat) and the corresponding standard deviations are 1.73 °C and 1.72 °C. The comparisons of the weekly averaged HY-2 RM and OI SST show that the biases of each week difference are from −1.06 °C to 0.48 °C with the mean value of −0.30 °C. The standard deviations of the SST difference are from 0.83 °C to 1.47 °C with the mean value of 1.05 °C. The relationships between SST difference and the sea surface and atmospheric parameters, such as wind speed, wind direction, SST, and water vapor are investigated.

Index Terms—Haiyang-2 (HY-2), scanning microwave radiometer (RM), sea surface temperature (SST).

I. INTRODUCTION

SEA surface temperature (SST) is an important ocean environmental parameter and an indicator of climate change, and is widely used in ocean dynamics, air–sea interaction, fisheries research, climatological forecast, and other fields. The passive infrared and microwave sensors can observe SST from space. Infrared sensors can measure SST with high resolution, but the observations are limited by cloud and aerosol contamination. In contrast to infrared measurements, microwave measurements can penetrate clouds and are less affected by aerosols [1]. Therefore, microwave radiometers

are capable of providing almost all-weather observations of SST. When rain is present, the microwave SST retrievals are not reliable, but the rain is easily detected and removed [2]. However, the spatial resolution of microwave measurements is relatively low compared with infrared measurements. Microwave SST retrieval was first attempted using the Scanning Multichannel Microwave Radiometer (SMMR) that was launched on Seasat and Nimbus-7 satellites in 1978. But the accuracy of SST measured by SMMR is low because of the poor calibration [1]. High-quality microwave SST data first became available in 1997 that was retrieved from measurements at 10.7 GHz by the Tropical Rainfall Measuring Mission Microwave Imager (TMI) with the root mean square (rms) difference between TMI and buoy SST ranging from 0.5 °C to 0.7 °C [1]. However, the SST accuracy of TMI retrievals decreases in cold water, approximately below 10 °C due to the degraded SST sensitivity of the 10.7-GHz brightness temperature with decreasing SST [3]. Moreover, TMI is in a low-inclination orbit that limits the field of view within 38° N–38° S. The TMI SSTs had a mean bias of −0.07 °C and a standard deviation of 0.57 °C when compared with the Tropical Atmosphere Ocean/Triangle Trans-Ocean Buoy Network (TRITON) and Pilot Research Moored Array in the Tropical Atlantic buoy SSTs [4]. Advanced Microwave Scanning Radiometer-Earth Observing System (AMSR-E) onboard Aqua satellite had operated during May 4, 2002 to October 4, 2011. AMSR-E SST retrievals are based on measurements of brightness temperature at 6.9 GHz, which overcome the restrictions of degraded SST accuracy in low temperatures at 10.7 GHz of TMI [3]. AMSR-E is the first polar orbiting microwave radiometer capable of measuring global SSTs since SMMR, eliminating the latitudinal sampling restriction of TMI [3], [5]. The AMSR-E version 7 SST products provided by remote sensing systems showed a small bias of −0.05 °C and a standard deviation of 0.48 °C, respectively, when compared with *in situ* SST observations [5]. Through three-way analysis between AATSR, AMSR-E, and *in situ* SST observations, AMSR-E version 5 SSTs showed an error of 0.42 K [6]. AMSR-E version 7 SST standard products provided by the Japan Aerospace Exploration Agency (JAXA) showed the mean difference of 0.207 °C and rms difference of 0.536 °C when compared with TRITON data [7].

The microwave SST measurements are currently available from on-orbit microwave radiometers, such as WindSat located on the Department of Defense Coriolis satellite launched in January 2003, and Advanced Microwave Scanning Radiometer-2 (AMSR2) onboard on Global Climate Observation Mission-Weather satellite launched in May 2012, and

M. Liu, L. Guan, and G. Chen are with the Department of Marine Technology, College of Information Science and Engineering, Ocean University of China, Qingdao 266100, China, and also with the Laboratory for Regional Oceanography and Numerical Modeling, Qingdao National Laboratory for Marine Science and Technology, Qingdao 266071, China (e-mail: leiguan@ouc.edu.cn).

W. Zhao is with the National Satellite Ocean Application Center, State Oceanic Administration, Beijing 100081, China.

Color versions of one or more of the figures in this paper are available online at http://ieeexplore.ieee.org.

the Global Precipitation Measurement (GPM) Microwave Radiometer (GMI) onboard on GPM satellite launched in February 2014. The WindSat radiometer operates in five discrete channels, including 6.8, 10.7, 18.7, 23.8, and 37.0 GHz. The 10.7-, 18.7-, and 37.0-GHz channels are fully polarimetric, whereas the 6.8- and 23.8-GHz channels have only dual polarizations [8], [9]. The footprint size of 6.8-, 10.7-, 18.7-, 23.8-, and 37.0-GHz channels is 39 km × 71 km, 25 km × 38 km, 16 km × 27 km, 20 km × 30 km, and 8 km × 13 km, respectively. The WindSat version 7 SSTs showed a mean bias of −0.05 °C and 0.02 °C and a standard deviation of 0.55 °C and 0.52 °C for descending and ascending data, respectively, when compared with global telecommunication system (GTS) drifting buoy SST measurements during the period from June 2002 to December 2010 [10]. AMSR2 is an improved microwave radiometer compared with AMSR-E, with several improvements, including larger main reflector, additional channels at 7.3 GHz, and improved calibration system [11]. Remote Sensing Systems AMSR-2 version 7.2 SST data showed a mean bias of −0.04 K and a standard deviation of 0.55 K when compared with *in situ* observations during the period from July 2012 to October 2014 [12]. The AMSR2 version 1 SST standard product provided by JAXA showed mean difference of 0.218 °C and an rms difference of 0.492 °C when compared with TRITON data from July 2012 to June 2013 [7]. GMI is a dual-polarization and conical-scanning passive microwave radiometer with multichannels ranging from 10.65 to 183.31 GHz. GMI has exhibited highly accurate and stable calibration. The 10.7-GHz channel of GMI is available measure SST. Besides, GMI allows a full sampling of all local earth times repeated because the GPM satellite is in a 65° inclination nonsun-synchronous orbit [13]. GMI SST products by JAXA and remote sensing systems are available.

The Haiyang-2 (HY-2) is the first marine dynamic environmental satellite of China, launched on August 16, 2011. HY-2 satellite is in an altitude of 973-km sun-synchronous orbit with the local time of descending node at 6:00 A.M. It is used for all-weather conditions obtaining dynamic ocean environment parameters, such as sea surface wind field, sea surface height, significant wave height, and SST on a global scale [14]. It carried four microwave instruments, including a microwave scatterometer, radar altimeter, scanning microwave radiometer (RM), and three-frequency microwave radiometer. The RM onboard HY-2 is a multichannel radiometer capable of obtaining oceanic and atmospheric parameters, such as sea surface wind speed, SST, water vapor, and cloud liquid water under all-weather conditions [14]. It has nine channels and five frequencies, including 6.6, 10.7, 18.7, 23.8, and 37 GHz with both horizontal and vertical polarizations measured separately, except on the 23.8-GHz channel, which only operates with vertical polarization [14]. The footprint size of 6.6-, 10.7-, 18.7-, 23.8-, and 37-GHz channels is 75 km × 100 km, 50 km × 75 km, 25 km × 40 km, 25 km × 30 km, and 15 km × 25 km, respectively. The Earth incidence angle of HY-2 RM is 47.7° and the scan width is 1600 km [14]. The preliminary HY-2 RM SST products were compared with National Centers for Environmental Prediction reanalysis data

on a global scale from October 10 to October 20, 2011. The results showed that the rms is 2.0872 °C [14]. Zhao *et al.* [15] also assessed the initial SST products of HY-2 RM from January 2012 to June 2012 with the National Data of Buoy Center mooring and Argo buoy data. The results indicated that the accuracy of radiometer SST is better than 1.7 °C.

In this paper, the three-year HY-2 RM Level 2A (L2A) SST products from January 2012 to December 2014 are evaluated by buoy SST measurements, WindSat SST products, and National Oceanic and Atmospheric Administration (NOAA) Optimum Interpolation (OI) weekly SST products in order to analyze the accuracy, stability, and consistency of HY-2 RM SST products. The error dependencies of HY-2 RM SST on surface and atmospheric parameters are investigated. In Section II, the data sets used are introduced. In Sections III and IV, HY-2 RM SSTs are compared with buoy SST data, WindSat SSTs, and OI weekly averaged SSTs. In Section V, the error sources of HY-2 RM SST products are discussed. In Sections VI, the main results are summarized.

II. DATA SET

A. HY-2 RM Data

The HY-2 RM L2A products are developed and distributed in HDF format by National Satellite Ocean Application Service of State Oceanic Administration. Geophysical parameters are calculated based on the retrieval algorithm using Level 1B brightness temperatures, including SST at 6.6- and 10.7-GHz resolution, a sea surface wind speed at 10.7- and 18.7-GHz resolution, a water vapor at 18.7-GHz resolution, a cloud liquid water at 18.7-GHz resolution, an ice concentration at 18.7-GHz resolution, and a rain rate at 18.7-GHz resolution [14]. In this paper, the SST data at 6.6-GHz resolution are used.

B. WindSat Data

WindSat products used in this paper are provided by remote sensing systems. The products used in this paper are version 7.0.1 gridded binary daily data. Different geophysical parameters, including SST, sea surface wind speed and wind direction, rain rate, atmospheric water vapor, and cloud liquid water, are projected to 0.25° × 0.25° grid divided into two sets of maps based on ascending and descending passes. Daily data files contain Universal Time Coordinated observation time maps for each set of passes (descending and ascending).

C. NOAA OI Data

A weekly averaged OI SST analysis has been produced by NOAA with 1° spatial resolution using both *in situ* and satellite data from November 1981 to the present [16]. The products used for the comparisons in this paper are version 2.0 products. The *in situ* SST data are obtained in real time from GTS, including ship and buoy observations. The satellite SST data are from Advanced Very High Resolution Radiometer on the NOAA satellites [16]. The OI weekly products have been widely used for weather and climate monitoring and forecasting since 1993 [16].
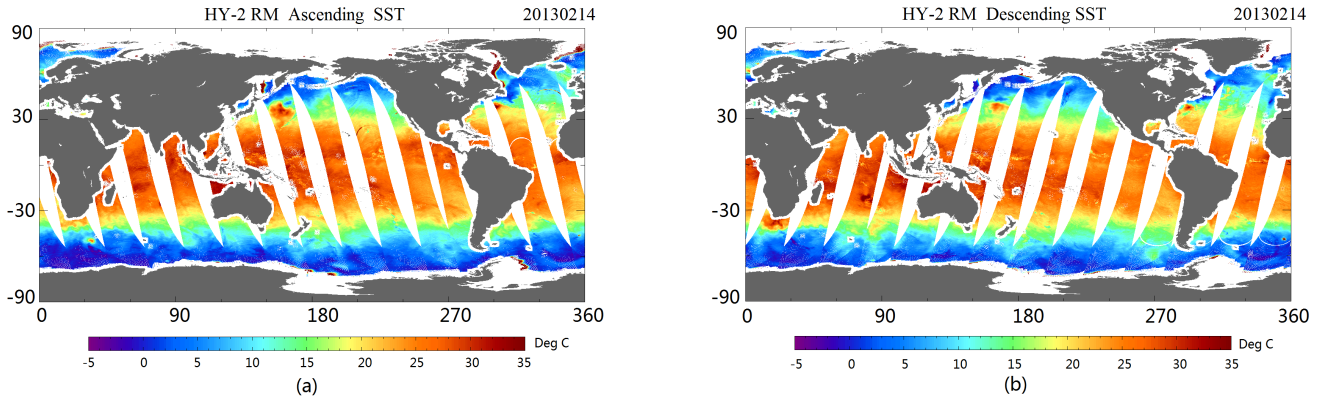
Fig. 1. HY-2 RM SST on February 14, 2013. (a) Ascending. (b) Descending.

D. NOAA iQuam In Situ Data

The *in situ* SST data used for evaluation are from the *in situ* SST Quality Monitor (iQuam) System, developed by National Environmental Satellite, Data, and Information Service, Center for Satellite Applications and Research, NOAA. The data are used to perform near real-time quality control of *in situ* measurements and to monitor the statistics [17]. Ships and buoys (drifters and moorings) are included but only buoy data are selected in this paper, considering the reliability and accuracy of *in situ* data [17]. The iQuam data files preserve all information from the original GTS data sets, including SST and other parameters, such as wind speed, wind direction, dew point temperature, and so on. iQuam monthly data files are served online in the HDF format. For this paper, the highest quality level data are selected.

III. COMPARISON OF HY-2/RM SST WITH BUOY AND WINDSAT SST DATA

The HY-2 RM L2A SST products are projected to daily ascending and descending equal-angle maps with a grid size of 0.25°. Fig. 1 shows daily projected HY-2 RM SST on February 14, 2013. WindSat and iQuam buoy SST data are used to evaluate the HY-2 RM SST products during the period from 2012 to 2014. The local time of ascending node of WindSat and HY-2 RM is both around 18:00. The collocations of HY-2 RM, WindSat, and buoy SST data are generated with the spatial window of 0.25° and the temporal window of 0.5 h. The overpass of WindSat and RM had missed the hottest time of the day and both sensors measure the same ocean layer at the same time of the day. The temporal window is 0.5 h for WindSat, RM, and buoy collocations. The diurnal warming effect is not significant in the comparisons among HY-2 RM, WindSat, and buoy. The statistics, including bias, median, standard deviation, robust standard deviation (RSD), and the proportion of SST difference, were calculated. The RSD used in this paper is 1.48 times the median absolute deviation from the median [18]. The outliers are removed using three times the RSD from the median [6], [19], [20]. The daily and three-year statistics are shown in Tables I and II. The left panel of Fig. 2 shows daily SST difference of HY-2 RM minus

TABLE I
DAILY STATISTICS OF SST DIFFERENCE BETWEEN HY-2 RM, WINDSAT, AND BUOY SST DATA FROM JANUARY 2012 TO DECEMBER 2014

	RM − buoy		RM-WindSat		WindSat - buoy	
	range	mean	range	mean	range	mean
Bias(°C)	-1.33–1.61	-0.38	-1.31–1.85	-0.33	-0.34–0.27	-0.05
Median(°C)	-1.40–1.07	-0.52	-1.47–1.17	-0.48	-0.33–0.20	-0.03
Std.Dev(°C)	0.88–3.62	1.69	0.76–3.49	1.68	0.31–0.81	0.52
RSD(°C)	1.01–4.34	1.93	0.88–4.20	1.92	0.35–0.91	0.59

buoy [Fig. 2(a)], HY-2 RM minus WindSat [Fig. 2(b)], and WindSat minus buoy [Fig. 2(c)], and the right panel shows the three-year SST difference of HY-2 RM minus buoy [Fig. 2(d)], HY-2 RM minus WindSat [Fig. 2(e)], and WindSat minus buoy [Fig. 2(f)]. For daily statistics, the blue line indicates the bias and the red vertical bars are the standard deviations. There are some missing values when the HY-2 RM data are invalid. Fig. 2(a) and (b) shows large standard deviations and fluctuating biases between HY-2 RM and buoy as well as HY-2 RM and WindSat comparisons. For the difference of HY-2 RM minus buoy SST, the biases range from −1.33 °C to 1.61 °C with the mean value of −0.38 °C and the standard deviations range from 0.88 °C to 3.62 °C with the mean value of 1.69 °C. In addition, the comparisons of HY-2 RM with WindSat show that the biases range from −1.31 °C to 1.85 °C with the mean value of −0.33 °C and the standard deviations range from 0.76 °C to 3.49 °C with the mean value of 1.68 °C. The daily statistics of the difference of WindSat minus buoy show small and smooth biases and standard deviations with the mean bias of −0.05 °C and the mean standard deviation of 0.52 °C. The overall three-year statistics of HY-2 RM with buoy and WindSat indicate the cold biases of −0.45 °C and −0.41 °C and relatively the large standard deviations of 1.73 °C and 1.72 °C. Moreover, the daily statistics patterns and three-year comparison results between HY-2 RM and buoy are similar to those between HY-2 RM and WindSat. The comparison of WindSat with buoy shows the bias of −0.03 °C and the standard deviation of 0.53 °C, which is consistent with the validation results given by Gentemann [10].

The three-way error analysis of the collocations of HY-2 RM, WindSat, and buoy SST data was carried out. The method was developed to estimate the standard deviation of
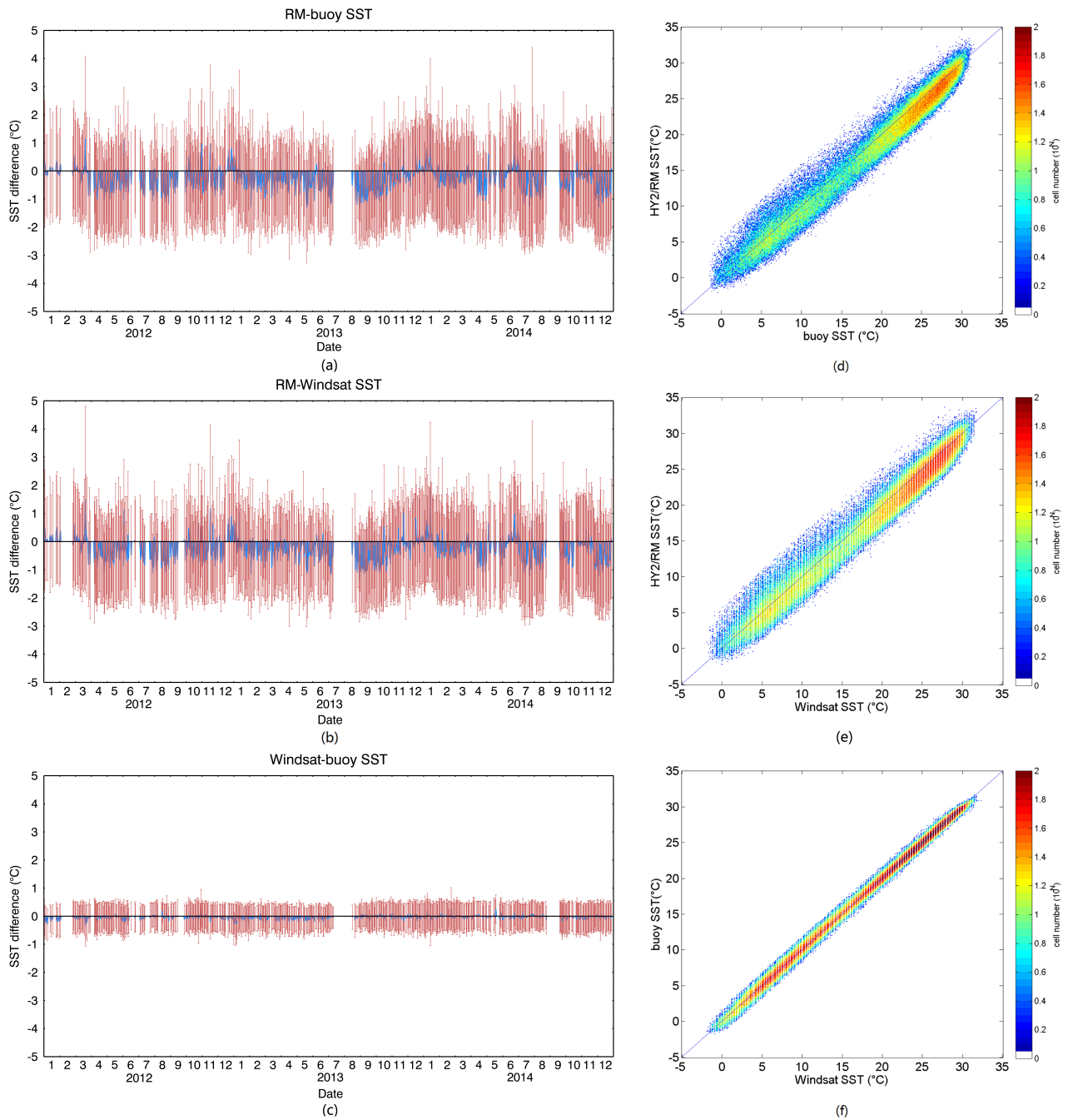
Fig. 2. Daily statistics (left panel) and three-year statistics (right panel) of the SST difference between (a) and (d) HY-2 RM and buoy, (b) and (e) HY-2 RM and WindSat, and (c) and (f) WindSat and buoy SST data.

TABLE II

THREE-YEAR STATISTICS OF SST DIFFERENCE BETWEEN HY-2 RM, WINDSAT, AND BUOY SST DATA FROM JANUARY 2012 TO DECEMBER 2014

	Number	Bias(°C)	Median(°C)	Std.Dev(°C)	RSD(°C)	P(±0.5°C)(%)	P(±1°C)(%)	P(±2°C)(%)
RM-buoy	166323	-0.45	-0.59	1.73	1.97	22.76	43.23	74.02
RM- WindSat	166323	-0.41	-0.56	1.72	1.97	22.92	43.31	74.48
WindSat -buoy	166323	-0.03	-0.03	0.53	0.59	68.37	92.62	100

different observation types [21]. O'Carroll *et al.* [6] evaluated SSTs from AATSR, AMSR-E, and *in situ* observations using the three-way error analysis. Gentemann [5] validated

MODIS, AMSR-E, and *in situ* SSTs using the three-way error analysis. The assumption of the analysis is that the errors in three observations are uncorrelated [6]. The variance of error
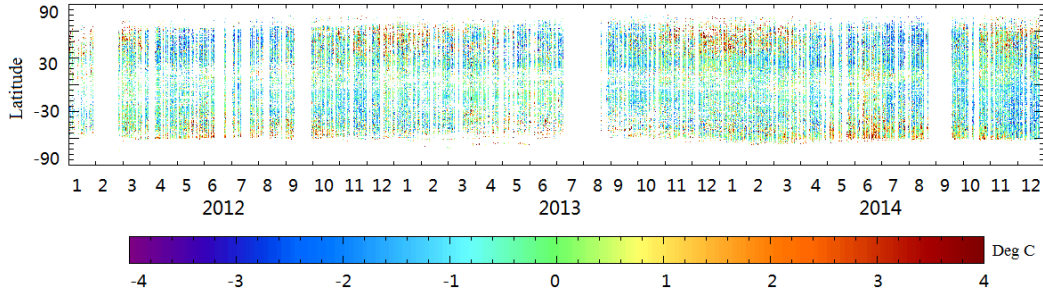
Fig. 3.   Latitude-time diagram of the daily difference of HY-2 RM minus buoy.
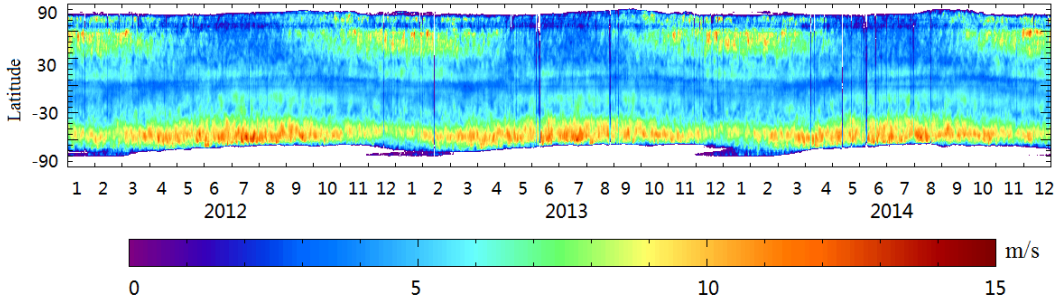

Fig. 4.   Latitude-time diagram of the sea surface wind speed from WindSat.

in each observation type can be calculated from the following equations [6]:

$$\sigma_1^2 = \frac{1}{2}(V_{12} + V_{31} - V_{23})$$

$$\sigma_2^2 = \frac{1}{2}(V_{23} + V_{12} - V_{31})$$

$$\sigma_3^2 = \frac{1}{2}(V_{31} + V_{23} - V_{12}) \qquad (1)$$

where 1–3 indicate the three different observation types and V_{ij} is the variance of difference between observation type i and j. σ_i^2 is the estimated error variance of observation type i. In this paper, subscripts 1–3 refer to HY-2 RM, WindSat, and buoy SST. The results indicate that the errors of these three observations are 1.68 °C for HY-2 RM, 0.36 °C for WindSat, and 0.38 °C for buoy SST. The buoy SST accuracy is consistent with the result given by Xu and Ignatov [22].

To understand the variation of the daily collocations, latitude-time distribution of the daily mean difference of HY-2 RM minus buoy SST averaged into 1° from January 2012 to December 2014 is shown in Fig. 3. The gaps in Fig. 3 mean no valid data. Fig. 4 is the latitude-time diagram of the WindSat daily surface wind speed from January 2012 to December 2014. In the mid- and high-latitude ocean of the Northern Hemisphere, it is obvious that the HY-2 RM SSTs are higher than buoy SSTs and the difference is larger than 3 °C during the period from November to March of the following year. In the southern ocean where strong westerly winds prevail, HY-2 RM SSTs are also higher than buoy SSTs during the period from April to October. The warmer bias regions are coincident with wind speeds higher than 8m/s. The SST difference between HY-2 RM and buoy data is within 1 °C in the near-
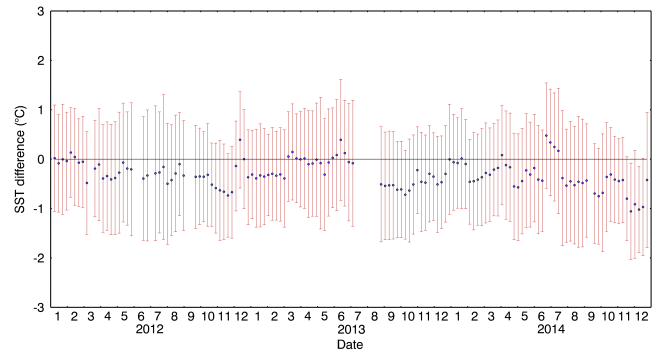

Fig. 5.   Weekly statistics of the SST difference between HY-2 RM and OI weekly averaged SST.

equatorial and low-latitude ocean where the wind speeds are low.

IV. COMPARISON OF HY-2 RM WITH OI WEEKLY AVERAGED SST

The HY-2 RM daily L2A SST products were averaged to 1° weekly averaged maps and compared with OI weekly SST data. Fig. 5 shows difference between HY-2 RM and OI weekly SST data from January 2012 to December 2014. The blue points indicate the biases of the weekly SST difference and the red vertical bars are the standard deviations. The biases are from −1.06 °C to 0.48 °C with the mean value of −0.30 °C. The standard deviations are from 0.83 °C to 1.47 °C with the mean value of 1.05 °C.

The bias and standard deviation of SST difference between HY-2 RM and OI weekly SST on each grid during the period from January 2012 to December 2014 were calculated.
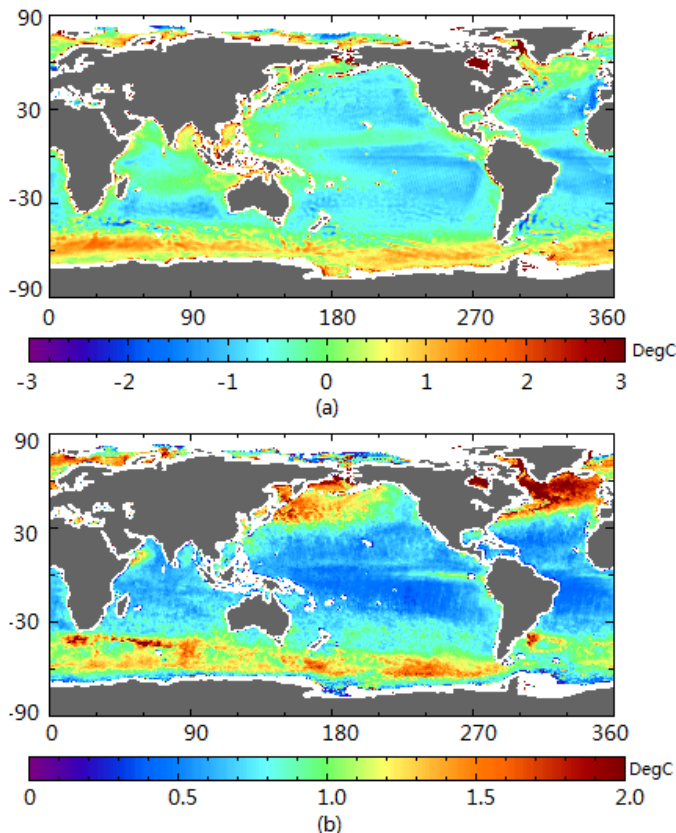
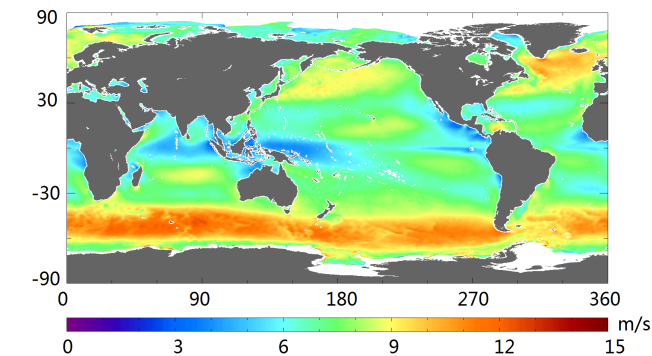Fig. 6. (a) Bias and (b) standard deviation of SST difference between HY-2 RM and OI weekly averaged SST.

Fig. 7. WindSat yearly averaged sea surface wind speed from 2012 to 2014.

Fig. 6(a) and (b) shows the global distribution of bias and standard deviation of SST difference, respectively. Fig. 7 is the averaged WindSat surface wind speed during the same period. Fig. 6(a) shows large warm bias in the southern ocean where strong westerly winds prevail. Moreover, HY-2 RM SSTs are colder than buoy SSTs within 1 °C in most of the near-equatorial and low-latitude ocean. Fig. 6(b) indicates that the standard deviations of SST difference are larger than 1 °C in the northern Atlantic and the northern Pacific where the wind speeds are relatively higher. The spatial patterns of the standard deviation of SST difference and the averaged wind speed are similar, indicating that SST disparity of HY-2 RM and OI is closely related to wind speed.

TABLE III
STATISTICS OF HY-2 RM MINUS BUOY SST FROM JANUARY 2012 TO DECEMBER 2014

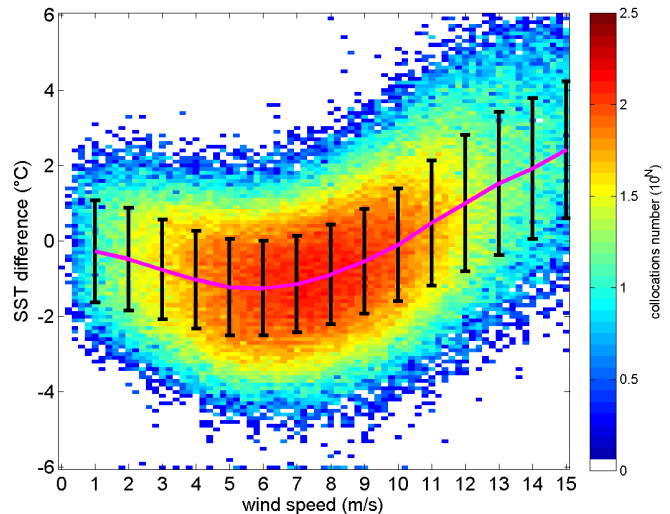|	Number	Bias(°C)	Std.Dev(°C)
Ascending	76354	-0.10	1.59
Descending	89969	-0.75	1.78
All	166323	-0.45	1.73

Fig. 8. Variation of SST difference against wind speed.

V. DISCUSSION

The comparisons of HY-2 RM SST with buoy, WindSat, and OI SST indicate large standard deviation and fluctuating biases of HY-2 RM SST. The error sources of HY-2 RM are discussed in this section.

The calibration procedure for microwave radiometer consists of two steps including: 1) transformation from radiometer counts of earth field to antenna temperature and 2) the antenna pattern correction that turns the antenna temperature to top of the atmosphere brightness temperature correcting for spillover effect and cross polarization coupling effect [23], [24]. The collocations between HY-2 RM and buoy data were separated according to HY-2 ascending and descending passes. The statistics were calculated. Table III shows that the biases are −0.10 °C and −0.75 °C and the standard deviations are 1.59 °C and 1.78 °C of ascending and descending collocations, respectively. The overall collocations show that the bias is −0.45 °C and the standard deviation is 1.73 °C (Table II). As discussed in [12], large biases between daytime and night-time measurements imply poor calibration of the satellite. The large difference of 0.65 °C between ascending and descending bias indicates that some problems exit in the calibration of HY-2 RM, such as the Earth radiation intrusion into cold mirror. Moreover, the daily statistics of SST difference between HY-2 RM and buoy show fluctuating biases and large standard deviations, implying that the HY-2 RM is not well calibrated.

The collocated SST difference and WindSat surface wind speed were further analyzed. Fig. 8 presents the variation of SST difference (RM minus buoy) against wind speeds. The background color indicates the number of collocations in every 0.2-m/s wind speed bin and in 0.1 °C SST difference bin. The
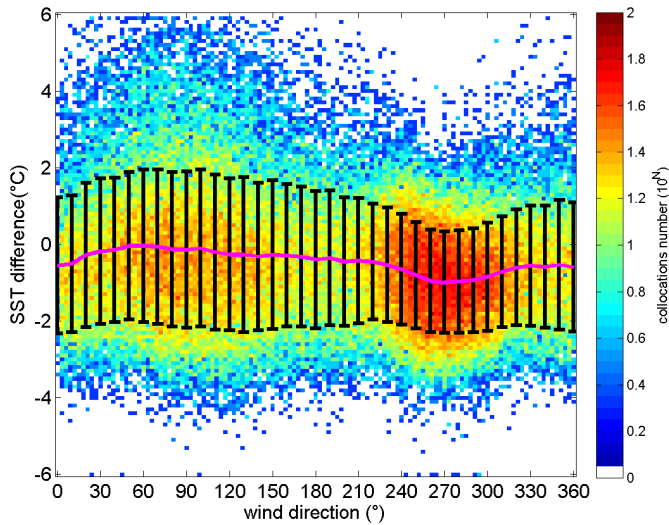
Fig. 9. Variation of SST difference against wind direction.

Fig. 10. Variation of SST difference against SST.

purple solid line shows the bias and the black vertical bars indicate the standard deviation of the SST difference in wind speed bin of 1 m/s. The biases are low in low wind speed range and become larger with high wind speeds. The biases are negative with the wind speeds lower than 10 m/s. The smallest standard deviation appears when wind speed is around 6 m/s and the biases and standard deviations increase with the increasing wind speeds, which is consistent with the results shown in Sections III and IV. In addition, the relationship between SST difference and wind speeds from the Advanced Scatterometer (ASCAT) is also analyzed. The results are similar to these using WindSat wind speed. The main reason for the error is that the sea surface emissivity in high wind speed has larger error. The surface roughness in terms of wind-induced emissivity is a function of wind speed and wind direction [23], [25]. The correlation between the emissivity and wind speed is not perfect leading to an error [25]. The uncertainty in surface emissivity because of wind speed effects becomes one of the main sources of known error in SST retrieval.

The relationship of SST difference and wind direction is shown in Fig. 9. Considering relatively larger error of WindSat wind direction in lower wind speeds [26], the collocated SST difference and WindSat direction were analyzed only using wind speeds higher than 5 m/s. The background color indicates the number of collocations in every 3° wind direction bin and in 0.1 °C SST difference bin. The purple solid line shows that the bias and the black vertical bars indicate the standard deviations in a wind direction bin of 10°. The results indicate the larger standard deviations of approximately 2 °C when wind directions are from 50° to 150°. Moreover, the standard deviations are lower than 1.5 °C when wind directions are from 240° to 320°. The relationship between SST difference and wind directions from ASCAT are also analyzed. The results are similar to these using WindSat wind direction. The microwave radiation emitted from the wind-roughed sea surface shows obvious correlated signature with respect to the wind direction relative to the radiometer azimuth [28]. The
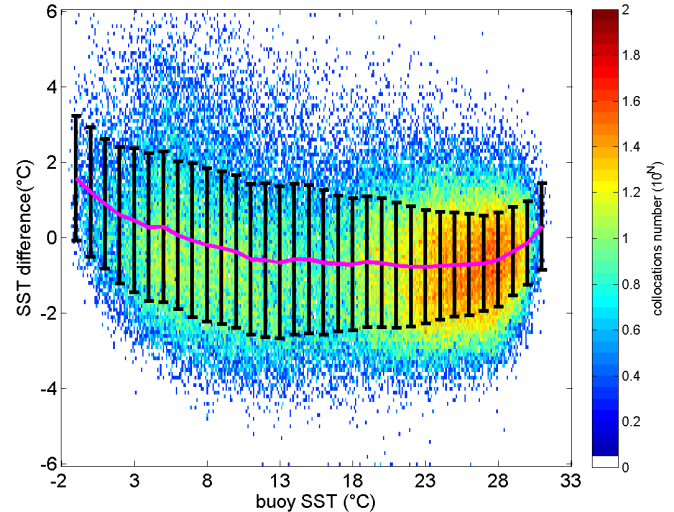
wind direction signal grows with wind speed and the amplitude of the wind direction signal is approximately proportional to wind speed [25], [27], [28]. This leads to a significant error in the retrieved SST.

The relationship between SST difference and SST was also investigated. Fig. 10 shows the results. The background color indicates the number of collocations in 0.2 °C SST bin and in 0.1 °C SST difference bin. The purple solid line shows the bias and the black vertical bars indicate the standard deviation of the SST difference in SST bin of 1 °C. The results indicate larger biases and standard deviations with lower SSTs. The biases decrease when SSTs increase, from 2 °C in the cold waters to about −0.5 °C under most of the SST values. The standard deviations are around 2 °C and decrease to smaller value in warmer waters. Gentemann *et al.* [2] presented the sensitivity of 7-GHz vertical polarized measurements to SST. The results showed that the sensitivities of 7-GHz vertical polarization brightness temperature to SST are 0.39, 0.59, and 0.65 with the SST of 0 °C, 15 °C, and 30 °C, respectively. Shibata [29] obtained the relation between the sea surface brightness temperature of 6-GHz vertical polarization and 6-GHz horizontal polarization and the SST. Through the relation curve, it is obvious that brightness temperature is more sensitive to SST in warm water than in cold water. The decreasing sensitivity of brightness temperature to SST in cold water leads to larger error in SST retrieval.

The relationship of SST difference and atmospheric water vapor is shown in Fig. 11. The background color indicates the number of collocations in 1-mm atmospheric water vapor bin and in 0.1 °C SST difference bin. The purple solid line shows the bias and the black vertical bars indicate the standard deviation of the SST difference in atmospheric water vapor bin of 2 mm. The results show larger biases and standard deviations with lower atmospheric water vapors. The biases are positive with atmospheric water vapors lower than 10 mm. The standard deviations are around 2 °C and decrease to smaller value in higher atmospheric water vapors. In the microwave
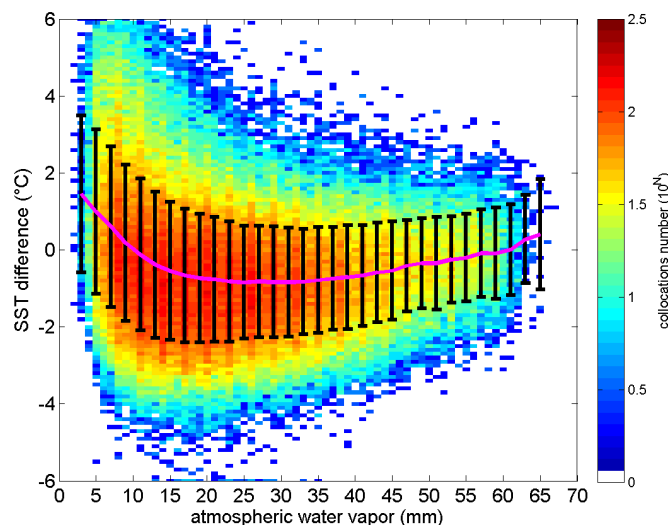
Fig. 11. Variation of SST difference against atmospheric water vapor.

spectrum below 100 GHz, atmospheric absorption is due to oxygen, water vapor, and liquid water [30]. The main reason of larger errors in lower water vapors is the atmospheric absorption model errors [31].

VI. CONCLUSION

The HY-2 RM L2A SST products are evaluated by comparing with the buoy, WindSat, and OI weekly averaged SST during the period from January 2012 to December 2014. The biases are −0.45 °C (RM minus buoy) and −0.41 °C (RM minus WindSat) and the standard deviations are 1.73 °C and 1.72 °C when compared with buoy and WindSat SST, respectively. The comparisons of weekly averaged SST between HY-2 RM and OI show that the biases of each week are between −1.06 °C and 0.48 °C and the standard deviations are between 0.83 °C and 1.47 °C. The SST difference is much higher in the regions of the Northern Pacific Ocean, the Northern Atlantic Ocean, and the Southern Ocean where strong winds prevail.

The results indicate large standard deviation and fluctuating biases of HY-2 RM SST. The relatively large difference between ascending and descending comparisons and the fluctuating biases and large standard deviations indicate that HY-2 RM is not well calibrated. The relationships between SST difference and the sea surface and atmospheric parameters, such as wind speed, wind direction, SST, and water vapor, are investigated. The biases and standard deviations increase with the increasing of wind speeds. There is dependency of SST difference on wind directions. The error is larger in cold water because of decreasing sensitivity of brightness temperature to SST. The biases and standard deviations are larger with lower atmospheric water vapors. The calibration and the retrieval algorithm of HY-2 RM need to be improved in the future.

REFERENCES

[1] F. J. Wentz, C. Gentemann, D. Smith, and D. Chelton, "Satellite measurements of sea surface temperature through clouds," *Science*, vol. 288, no. 5467, pp. 847–850, May 2000.

[2] C. L. Gentemann, T. Meissner, and F. J. Wentz, "Accuracy of satellite sea surface temperatures at 7 and 11 GHz," *IEEE Trans. Geosci. Remote Sens.*, vol. 48, no. 3, pp. 1009–1018, Mar. 2010.

[3] D. B. Chelton and F. J. Wentz, "Global microwave satellite observations of sea surface temperature for numerical weather prediction and climate research," *Amer. Meteorol. Soc.*, vol. 86, no. 8, pp. 1097–1115, Aug. 2005.

[4] C. L. Gentemann, F. J. Wentz, C. A. Mears, and D. K. Smith, "*In situ* validation of tropical rainfall measuring mission microwave sea surface temperatures," *J. Geophys. Res.*, vol. 109, no. C4, C04021, Apr. 2004, doi: 10.1029/2003JC002092.

[5] C. L. Gentemann, "Three way validation of MODIS and AMSR-E sea surface temperatures," *J. Geophys. Res. Oceans*, vol. 119, no. 4, pp. 2583–2598, Apr. 2014.

[6] A. G. O'Carroll, J. R. Eyre, and R. W. Saunders, "Three-way error analysis between AATSR, AMSR-E, and *in situ* sea surface temperature observations," *J. Atmos. Ocean. Technol.*, vol. 25, no. 7, pp. 1197–1207, Jul. 2008.

[7] T. Hihara, M. Kubota, and A. Okuro, "Evaluation of sea surface temperature and wind speed observed by GCOM-W1/AMSR2 using *in situ* data and global products," *Remote Sens. Environ.*, vol. 164, pp. 170–178, Jul. 2015.

[8] P. W. Gaiser *et al.*, "The WindSat spaceborne polarimetric microwave radiometer: Sensor description and early orbit performance," *IEEE Trans. Geosci. Remote Sens.*, vol. 42, no. 11, pp. 2347–2361, Nov. 2004.

[9] W. E. Purdy, P. W. Gaiser, G. A. Poe, E. A. Uliana, T. Meissner, and F. J. Wentz, "Geolocation and pointing accuracy analysis for the WindSat sensor," *IEEE Trans. Geosci. Remote Sens.*, vol. 44, no. 3, pp. 496–505, Mar. 2006.

[10] C. L. Gentemann, "Microwave sea surface temperatures for climate," presented at the WCRP OSC Climate Res. Service Soc., Oct. 2011. [Online]. Available: http://www.wcrp-climate.org/conference2011/posters/C14/C14_Gentemann_T45B.pdf

[11] K. Imaoka, M. Kachi, M. Kasahara, N. Ito, K. Nakagawa, and T. Oki, "Instrument performance and calibration of AMSR-E and AMSR2," *Int. Arch. Photogram., Remote Sens. Spatial Inf. Sci.*, vol. 38, no. 8, pp. 13–16, 2010.

[12] C. L. Gentemann and K. A. Hilburn, "*In situ* validation of sea surface temperatures from the GCOM-W1 AMSR2 RSS calibrated brightness temperatures," *J. Geophys. Res. Oceans*, vol. 120, no. 5, pp. 3567–3585, May 2015.

[13] D. W. Draper, D. A. Newell, F. J. Wentz, S. Krimchansky, and G. M. Skofronick-Jackson, "The global precipitation measurement (GPM) microwave imager (GMI): Instrument overview and early on-orbit performance," *IEEE J. Sel. Topics Appl. Earth Observ. Remote Sens.*, vol. 8, no. 7, pp. 3452–3462, Jul. 2015.

[14] X. Jiang *et al.*, "The HY-2 satellite and its preliminary assessment," *Int. J. Digit. Earth*, vol. 5, no. 3, pp. 266–281, May 2012.

[15] Y. Zhao *et al.*, "Assessment of the initial sea surface temperature product of the scanning microwave radiometer aboard on HY-2 satellite," *Acta Oceanol. Sin.*, vol. 33, no. 1, pp. 1–5, 2014.

[16] R. W. Reynolds, N. A. Rayner, T. M. Smith, D. C. Stokes, and W. Wang, "An improved *in situ* and satellite SST analysis for climate," *J. Clim.*, vol. 15, no. 13, pp. 1609–1625, Jul. 2002.

[17] F. Xu and A. Ignatov, "*In situ* SST quality monitor (iQuam)," *J. Atmos. Ocean. Technol.*, vol. 31, no. 1, pp. 164–180, Jan. 2014.

[18] O. Embury, C. J. Merchant, and G. K. Corlett, "A reprocessing for climate of sea surface temperature from the along-track scanning radiometers: Initial validation, accounting for skin and diurnal variability effects," *Remote Sens. Environ.*, vol. 116, no. 4, pp. 62–78, Jan. 2012.

[19] P. Dash *et al.*, "Group for high resolution sea surface temperature (GHRSST) analysis fields inter-comparisons—Part 2: Near real time Web-based level 4 SST quality monitor (L4-SQUAM)," *Deep Sea Res. II, Topical Stud. Oceanogr.*, vols. 77–80, pp. 31–43, Nov. 2012.

[20] P. R. Bevington and D. K. Robinson, "Estimates of mean and errors," in *Data Reduction and Error Analysis for the Physical Sciences*, 3rd ed. New York, NY, USA: McGraw-Hill, 2003, p. 55.

[21] A. Stoffelen, "Toward the true near-surface wind speed: Error modeling and calibration using triple collocation," *J. Geophys. Res.*, vol. 103, no. C4, pp. 7755–7766, Apr. 1998.

[22] F. Xu and A. Ignatov, "Evaluation of *in situ* sea surface temperatures for use in the calibration and validation of satellite retrieval," *J. Geophys. Res. Oceans*, vol. 115, no. C9, p. C09022, Sep. 2010, doi: 10.1029/2010JC006129.

[23] T. Meissner and F. J. Wentz, "The emissivity of the ocean surface between 6 and 90 GHz over a large range of wind speeds and earth incidence angles," *IEEE Trans. Geosci. Remote Sens.*, vol. 50, no. 8, pp. 3004–3026, Aug. 2012.

[24] T. Meissner, F. J. Wentz, and D. Draper, "GMI calibration algorithm and analysis theoretical basis document, version F," Remote Sens. Syst., Santa Rosa, CA, USA, Tech. Rep. 111311, 2011.

[25] F. J. Wentz, "A well-calibrated ocean algorithm for special sensor microwave/imager," *J. Geophys. Res.*, vol. 102, no. C4, pp. 8703–8718, Apr. 1997.

[26] F. J. Wentz, T. Meissner, and D. K. Smith, "Assessment of the WindSat retrievals produced by NRL," Remote Sens. Syst., Santa Rosa, CA, USA, Tech. Rep. 010605, Jan. 2005.

[27] F. J. Wentz and T. Meissner, "Supplement 1: Algorithm theoretical basis document for AMSR-E ocean algorithms," Remote Sens. Syst., Santa Rosa, CA, USA, Tech. Rep. 051707, May 2007.

[28] T. Meissner and F. Wentz, "An updated analysis of the ocean surface wind direction signal in passive microwave brightness temperatures," *IEEE Trans. Geosci. Remote Sens.*, vol. 40, no. 6, pp. 1230–1240, Jun. 2002.

[29] A. Shibata, "Features of ocean microwave emission changed by wind at 6 GHz," *J. Oceanogr.*, vol. 62, no. 3, pp. 321–330, Jun. 2006.

[30] F. J. Wentz and T. Meissner, "Algorithm theoretical basis document (ATBD) version 2 AMSR ocean algorithm," Remote Sens. Syst., Santa Rosa, CA, USA, Tech. Rep. 121599A-1, Nov. 2000.

[31] F. J. Wentz and T. Meissner, "Atmospheric absorption model for dry air and water vapor at microwave frequencies below 100 GHz derived from spaceborne radiometer observations," *Radio Sci.*, vol. 51, no. 5, pp. 381–391, May 2016.

Mingkun Liu (S'15) received the B.S. degree in marine technology from the Ocean University of China, Qingdao, China, in 2014, where she is currently pursuing the Ph.D. degree in ocean remote sensing.

Her research interests include validation and retrieval of sea surface temperature from satellite infrared and microwave radiometers.

Lei Guan (M'05) received the B.S. degree in electronic engineering and the Ph.D. degree in marine physics from the Ocean University of China (OUC), Qingdao, China, in 1992 and 1998, respectively.

She has been with the OUC since 1998, where she has been involved in research and teaching. She is currently a Professor with the Department of Marine Technology, College of Information Science and Engineering, OUC. She visited Tohoku University, Sendai, Japan, where she conducted research from 2000 to 2001. Her current research interests include remote sensing of the oceanic parameters, primarily in the retrieval, validation, and merging of multisensor sea surface temperature (SST).

Dr. Guan has been a member of the Group for High Resolution SST Science Teams since 2011. She has been a Principal Investigator for the national projects related with SST studies and involved in the international projects, such as the EC FP6 DRAGONESS Project, the China/ESA Dragon Project, and the IOC/WESTPAC New Generation SST Project. She advises graduate students and teaches undergraduate and graduate courses on digital image processing, introduction to atmospheric science, atmospheric radiative transfer, and Interactive Data Language (IDL) programming for satellite data processing.

Wei Zhao received the M.S. degree in optical science from the Anhui Institute of Optics and Fine Mechanics, Chinese Academy of Sciences, Beijing, China, in 2002, and the Ph.D. degree in atmospheric remote sensing from the Institute of Atmospheric Physics, Chinese Academy of Sciences in 2012.

She has been with the National Ocean Satellite Application Center, State Oceanic Administration, Beijing, since 2002, where she has been involved in the calibration and data processing for ocean color satellites.

Ge Chen received the B.S. degree in marine physics, the M.S. degree in satellite oceanography, and the Ph.D. degree in physical oceanography from the Ocean University of China (OUC), Qingdao, China, in 1988, 1990, and 1993, respectively.

He was a Post-Doctoral Fellow with the French Research Institute for Exploitation of the Sea, Brest, France, from 1994 to 1996. Since 1997, he has been a Professor of Satellite Oceanography and Meteorology with OUC. He has been the Dean of the College of Information Science and Engineering, OUC since 2004. He has authored over 80 peer-reviewed scientific papers published in internationally recognized journals. His current research interests include satellite remote sensing of the ocean and atmosphere and its application to climate change, marine geographical information system, and ocean big data mining.

Dr. Chen is a member of the Expert Committee on Ocean Technology for the National High Technology Program (the 863 Program) of China nominated by the Chinese Ministry of Science and Technology. In 2001, he received the National Science Funding for Outstanding Young Scientists by the Natural Science Foundation of China. He served as the Executive Secretary of the International Pan Ocean Remote Sensing Conference Association from 1998 to 2002. He became the Chair Professor of the Cheung Kong Scholars Program nominated by the Chinese Ministry of Education.